Journal of Basic Physical Research ISSN: 2141-8403 Prints, 2141-8411 Online
Vol.14, Issue 1, March, 2025, pp. 77 – 90, Available online at https://journals.unizik.edu.ng/jbpr/

ARRHENIUS-CONTROLLED FLUID FLOW OVER A SUPERHYDROPHOBIC MICROCHANNEL WITH SYMMETRIC WALL CONCENTRATION

Emmanuel Omokhuale[1] and Godwin Ojemeri[2]
[1]*Department of Mathematical Science, Faculty of Sciences, Federal University Gusau, P. M. B. 1001, Zamfara State.*
[2]*Department of Mathematics, College of Sciences, Federal University of Agriculture, Zuru, P. M. B. 28, Kebbi State, Nigeria.*

Abstract: *This paper demonstrates the effect of wall concentration on a magnetized heat and mass transfer flow affected by Arrhenius kinetics in a slit microchannel. One of the parallel plates is intentionally modified to have a superhydrophobic surface (SHS), while the other plate has a no-slip surface (NSS). The nonlinear ordinary differential equations are treated with the regular perturbation method. The actions of key parameters controlling the flow behavior in terms of momentum and energy distributions are illustrated graphically. The present study is valid for the limiting case because it is based on a comparison with earlier studies that back it up. It was revealed that the existence of symmetric wall concentration substantially influences flow development and reversal. This research will have applications relevant to cracking in petrochemical engineering, chemical synthesis, anti-wetting micro-technology, etc.*

Keywords: *Mass flow, Symmetric wall concentration, Arrhenius kinetics, Magnetohydrodynamics (MHD), Superhydrophobic Microchannel.*

Introduction

The study of electrically conductive liquids, such as plasma, electrolytes, salt water, and liquid metals, is called magnetohydrodynamics (MHD). There are numerous technical and commercial applications for this type of liquid, including magnetic drug targeting, crystal formation, power generation, reactor cooling, and MHD sensors (Jawad *et al*. 2021). Hartmann and Lazarus (1937) were the first to conduct an experimental study of modern MHD flow in laboratories. This research laid the groundwork for the creation of numerous MHD devices, including MHD pumps, MHD generators, brakes, flow meters, and geothermal-powered energy extraction. Afterwards, numerous researches have been published to analyze the effects of MHD free convection along different flow media. In view of this, Onwubuya and Ojemeri (2023) performed a comparative analysis of MHD mixed convection with a thermal radiation factor in an upstanding porous channel using a homotopy perturbation approach. Hamza *et al*. (2023) explained the impact of hydromagnetic natural convection flow on a chemically reacting fluid affected by symmetric and asymmetric heating conditions using the homotopy perturbation approach. Jha *et al*. (2023) modelled the buoyancy-induced magnetic field flow of a fluid in an upright plate with point/line heat sink/source at various channel locations. Hydromagnetic Casson nanofluidic flow for mass and heat transport through a stretching plate was studied by Saeed and Gul (2021). The consequences of cross-diffusion on non-Newtonian fluid flow over an extended range employing an unequal heat sink/source were researched by Reddy *et al*. (2018). The Fehlberg approach was employed in this analysis to get the answer to the modeled problem. The joint functions of fractional and non-uniform heat on the flow regime were investigated by the authors. The actions of heat absorption/generation and chemical reaction on the Maxwell magnetized nanofluid flux were discussed by Sravanthi and Gorla (2018). The authors used the semi-analytical and homotopy analysis methods to solve the formulated model in this problem by considering flow over an extended surface with exponential convection. Ojemeri *et al*. (2023a) deliberated on the hydromagnetic flux of an electrically conducting non-Newtonian liquid instigated by the radiative factor in an upright

porous channel. References like Rostami *et al.* (2021), Obalalu *et al*. (2021), and Uygun *et al*. (2022) shed more light on this phenomenon.

In heat transfer problems with MHD effect, the study of fluid flow in microchannels with superhydrophobic (SHO) characteristics and jump temperature is a novel area of growing interest. Some of the features of microchannels with SHS are extreme water repellent, self-cleaning mechanisms, reduced friction, and enhanced flow. According to Lee *et al*. (2021), microchannels with SHS can minimize the effect of water exposure on surfaces and enable self-cleaning behavior. Microchannels with SHS found applications in the development of lab-on-a-chip devices for medical diagnostics, heat transfer enhancement by allowing for efficient liquid flow, controlled microfluidic transport, and separating oil and water in microfluidic systems. A number of researchers have accomplished their work on the above subject. Akhtari and Karimi (2020) mentioned that SHS applied to microchannels can minimize the pumping power needed for instigating fluid flow. Several outstanding scholars have greatly contributed to the studies of different effects in microchannels influenced by SHS. To this end, Hamza *et al*. (2025) recently investigated the significance of dusty fluid in unsteady fractional derivatives in Caputo-Fanrizio (CF) and Atangana-Baleanu in Caputo sense (ABC) in addressing heat transfer problem through a SHO microchannel. Additionally, Hamza *et al*. (2024a, 2024b) reported the influence of electrokinetic effects on free and mixed convection flows in SHO microchannels and the temperature jump scenario. It is concluded from their computational analysis that the function of the SHS and electrokinetic effects is to enhance the fluid velocity in the microchannel. In the field of MHD, Ojemeri and Onwubuya (2023a) emphasized on the significance of magnetized mixed flow with porous medium in a slit microchannel. Jha and Gwandu (2018) and Jha and Gwandu (2020) studied fluid flow in the application of a magnetic field in an upstanding slit microchannel with SHS, porous material, and a temperature jump. Sharma *et al*. (2020) provided a mathematical model that describes the pressure-induced flow across a microchannel involving textured SHS with constant heat flux. Other interesting research with different thermal boundary conditions in the presence of SHS can be seen in these references Sia *et al*. (2023), Heidarian *et al*. (2020), and Zhang *et al*. (2019).

Arrhenius-controlled heat transfer (exothermic chemical reaction) through microchannels and slit microchannels coated with SHO surfaces have been an area of recent research interest due to its applicability in engineering and chemical industries, for heat transfer advancement, biomedical devices, etc. Microchannels with SHS found applications in the development of lab-on-a-chip devices for medical diagnostics, heat transfer enhancement by allowing for efficient liquid flow, controlled microfluidic transport, and separating oil and water in microfluidic systems. To this end, Ojemeri *et al*. (2024) recently underscored the significance of heat-generating/absorbing fluid on Arrhenius-controlled heat flow in a SHO heated microchannel using a regular perturbation approach. Ojemeri and Onwubuya (2023b) examined mixed convection flow under the action of a porous medium and chemically propelled heat absorbing/generating fluid in a SHO microchannel. Later on, Ojemeri and Onwubuya (2023c) investigated the impact of magnetized free flow on Arrhenius-controlled transfer problem in a microchannel equipped with SHO characteristic and temperature jump condition using semi-analytic method. Hamza *et al.* (2023b) discussed the consequences of Arrhenius-controlled chemical reaction and Hall current on hydromagnetic free convection flow of an incompressible fluid along an upstanding microchannel subjected to appropriate boundary conditions using homotopy perturbation method. Hamza *et al*. (2023c) shed more light on the implications of hydromagnetic natural convection of a chemically reacting fluid using homotopy perturbation technique. It is concluded from their results that mounting level of Frank-Kamenetskii, representing the viscous heating term is noticed to encourage both the

thermal and hydromagnetic fluid. Ojemeri *et al.* (2023b) focused their search on the analytical treatment of Arrhenius-controlled fluid in an upright microchannel saturated with porous material using homotopy perturbation method (HPM) restricted to an appropriate boundary conditions. Their results showed that the variations of chemical reaction, Darcy number, rarefaction and wall-ambient temperature parameters substantially dictate the fluid flow and volume flow rate respectively. Ojemeri and Hamza (2022) put forth a computational treatment of an Arrhenius kinetically propelled heat generating/absorbing fluid in a microchannel.

Many chemical engineering processes such as polymer production, manufacturing of ceramics or glassware and food processing are made realistically possible when heat and mass transfer occur simultaneously in a novel physical geometry like slit micro structure. Moreover, the combined impacts of heat and mass with symmetric wall concentration across microchannels having superhydrophobic features on fluid flow have not been exhaustively studied. Thus, motivated by the above knowledge gap found in these literature review, the focus of this work is to improve on the work of Ojemeri and Onwubuya (2023c) by incorporating and investigating the novel interactions between heat and mass transfer, MHD, and Arrhenius kinetics in a superhydrophobic microchannel. The modelled nonlinear equations are treated with the regular perturbation method. The outcome of this paper will not only be essential for improving fluid flow in microchannels but would also serve as a guide for the design of advanced thermal and mass management systems for microfluidic devices and high-performance applications. Additionally, the outcome of this study would play an important role in chemical industry, power and cooling industry for drying, chemical vapor deposition on surfaces, cooling of nuclear reactors and petroleum industries.

Mathematical Formulation

Imagine a steady magnetized flow of an incompressible fluid passing through two vertical parallel plates affected by Arrhenius kinetics and symmetric wall concentration conditions. As shown in Figures 1, the wall at $y_0 = 0$, is instigated by the extremely difficult to wet known as the SHO effect while the NSS is kept at $y_0 = L$. A transversely applied magnetic field of intensity B_0 is said to introduced within two upstanding microchannel plates. All the fluid properties are assumed to be constants. The flow variables are functions of space y only. In view of the present formulation, the following assumptions are further made:

- The fluid is laminar and incompressible.
- The flow is fully developed and obeys the Bousinesq's approximation.
- It is assumed that the fluid is influenced by Arrhenius kinetics.
- The fluid is assumed to be affected by symmetric wall concentration.

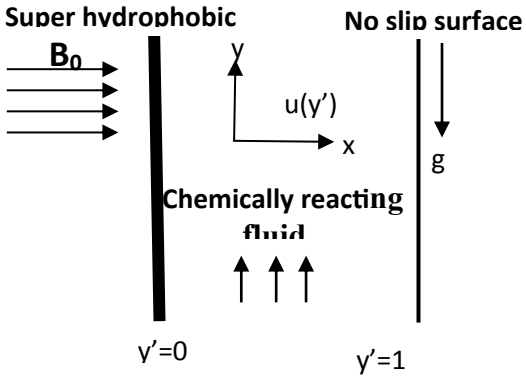


Figure 1: Physical Configuration of the Flow

Following Ojemeri and Onwubuya (2023c) and Hamza *et al*. (2024c), the present problem in dimensional form can be written as:

$$V\frac{d^2u'}{dy'^2} + g\beta_0(T' - T_O) + g\beta_1(C' - C_O) - \frac{\sigma B_O^2 u'}{\rho} = 0 \quad (1)$$

$$\frac{k}{\rho c_\rho}\frac{d^2T'}{dy'^2} + \frac{QC_0^* A}{\rho c_\rho} e^{\left(\frac{-E}{RT'}\right)} = 0 \quad (2)$$

$$D\frac{d^2C'}{dy'^2} = 0 \quad (3)$$

Subject to the boundary conditions:

$$\left.\begin{array}{l} \left.\begin{array}{c} u(y') = \gamma'\frac{du'}{dy'} \\ T(y') = T_h + \Gamma'\frac{dT'}{dy'} \\ C' = C_w \end{array}\right\} at\ y' = 0 \\ \left.\begin{array}{l} u(y') = 0 \\ T(y') = T_o \\ C' = -C_w \end{array}\right\} at\ y' = L \end{array}\right\} \quad (4)$$

Introducing the dimensionless quantities as:

$$u = \frac{u'}{U}, y = \frac{y'}{h}, \theta = \frac{T' - T_0}{T_w - T_o}, x = \frac{x'v}{Uh^2}, M^2 = \frac{\sigma\beta_o^2 h^2}{\rho v}, (Z, \gamma, \Gamma) = (Z', \gamma', \Gamma')/h$$

$$C = \frac{C' - C_0}{C_w - C_o}, \mathrm{N} = \frac{g\beta^*(T_w - T_o)H^2}{vU}, \varepsilon = \frac{RT_0}{E}, \lambda = \frac{QC_0^* AEH^2}{RT_0^2} \quad (5)$$

Substituting equation (5) into equations (1-4), the basic equations of the temperature and velocity becomes:

$$\frac{d^2U}{dy^2} - M^2U = -T - \mathrm{NC} \quad (6)$$

$$\frac{d^2T}{dy^2} + \lambda e^{\frac{T}{1+\varepsilon T}} = 0 \quad (7)$$

$$\frac{d^2C}{dy^2} = 0 \quad (8)$$

The boundary conditions are:

$$C(y) = \xi_w, \quad \theta(y) = 1 + \Gamma\frac{d\theta}{dy}, \quad u(y) = \gamma\frac{du}{dy} \quad \text{at } y = 0 \quad (9)$$

$$C(y) = -\xi_w, \ \theta(y) = 0, \quad u(z) = 0 \quad \text{at } y = 1$$

where M is the magnetic parameter, N is the sustention parameter, λ is the viscous heating parameter, ε is the activation energy, ξ_w is the wall concentration parameter, Γ is the temperature jump parameter, and γ is the velocity slip parameter.

Solution Procedure

The coupled nonlinear governing equations is solved using regular perturbation method such that the solutions of the temperature and velocity is assumed as:

$$U = u_0 + \lambda(u_1) \tag{10}$$

$$T = t_0 + \lambda(t_1) \tag{11}$$

$$C = c_0 + \lambda(c_1) \tag{12}$$

Inserting eqns (8) and (9) into eqns (5) to (7), and taking the coefficients of λ^0 and λ, we derive the following system of ordinary differential equations with their corresponding boundary conditions as:

$$\lambda^0: \frac{d^2u_0}{dy^2} - \mathrm{M}^2u_0 = -t_0 - \mathrm{N}c_0 \tag{13}$$

$$\lambda: \frac{d^2u_1}{dy^2} - \mathrm{M}^2u_1 = -t_1 - \mathrm{N}c_1 \tag{14}$$

$$\lambda^0: \frac{d^2\theta_0}{dy^2} = 0 \tag{15}$$

$$\lambda: \frac{d^2\theta_1}{dy^2} + 1 + \theta_0 + (\frac{1}{2} - \varepsilon)\theta_0^2 = 0 \tag{16}$$

$$\lambda^0: \frac{d^2c_0}{dy^2} = 0 \tag{17}$$

$$\lambda: \frac{d^2c_1}{dy^2} = 0 \tag{18}$$

$$\left.\begin{array}{c} \lambda^0: \theta_o = 1 + \Gamma\frac{d\theta_o}{dz} \\ \lambda: \theta_1 = \Gamma\frac{d\theta_1}{dz} \\ \lambda^0: u_0 = \gamma\frac{dU_o}{dz} \\ \lambda: u_1 = \gamma\frac{dU_1}{dz} \\ \lambda^0: c_0 = \xi_w \\ \lambda: c_1 = 0 \end{array}\right\} \text{at } z = 0 \tag{19}$$

and

$$\left.\begin{array}{c} \lambda^0: \theta_0 = 0 \\ \lambda: \theta_1 = 0 \\ \lambda^0: u_0 = 0 \\ \lambda: u_1 = 0 \\ \lambda^0: c_0 = -\xi_w \\ \lambda: c_1 = 0 \end{array}\right\} \text{at } z = 1 \tag{20}$$

The solutions of temperature and velocity is derived as:

$$c_0 = D_1z + D_2 \tag{21}$$

$$c_1 = 0 \tag{22}$$

$$\theta_0 = J_1z + J_2 \tag{23}$$

$$\theta_1 = -\frac{z^2}{2} - J_1\frac{z^6}{3} - J_2\frac{z^2}{2} - a_1(J_1^2\frac{z^4}{12} + J_1J_2\frac{z^3}{3} + J_2^2\frac{z^2}{2} + J_3z + J_4) \tag{24}$$

$$u_0 = J_5 \cosh(Mz) + J_6 sinh(\mathrm{Mz}) + J_7 z + J_8 \quad (25)$$

$$u_1 = J_{10} \cosh(Mz) + J_{11} sinh(\mathrm{Mz}) + J_{12} z^5 + J_{13} z^4 + J_{14} z^3 + J_{15} z^2 + J_{16} z + J_{17} \quad (26)$$

where the heat transfer rate and shearing stress is derived as:

$$\frac{dC}{dy}\Big|_{y=0} = D_1 \quad (27)$$

$$\frac{dC}{dy}\Big|_{y=1} = D_1 \quad (28)$$

$$\frac{d\theta}{dy}\Big|_{y=0} = J_1 + \lambda J_3 \quad (29)$$

$$\frac{d\theta}{dy}\Big|_{y=1} = J_1 + \lambda\left[-2J_1 - 2J_2 - a_1\left(\frac{J_1^2}{3} + J_1 J_2 + J_2^2 + J_3\right)\right] \quad (30)$$

$$\frac{dU}{dy}\Big|_{y=0} = MJ_6 + J_8 + \lambda[MJ_{11} + J_{16}] \quad (31)$$

$$\frac{dU}{dy}\Big|_{z=1} = MJ_5 \sinh(\mathrm{M}) + MJ_6 \cosh(M) + J_8 + \lambda[MJ_{10} \sinh(\mathrm{M}) + MJ_{11} \cosh(\mathrm{M}) + 5J_{12} + 4J_{13} + 3J_{14} + 2J_{15} + J_{16}] \quad (32)$$

Where all the constants are defined in the appendix

Results and Discussion

The interaction of Arrhenius-driven heat transfer flow with symmetric wall concentration impact over a microchannel coated SHS and temperature jump characteristics is performed analytically. A semi-analytical method is employed to treat the resultant steady ordinary differential equations. Some graphs have been plotted to demonstrate the effect of pertinent parameters. The default values chosen for this analysis are ($\gamma = \Gamma = 1$, N =5, ξ_w=0.1, M=0.5, λ = 0.001).

Figure 2 is sketched to demonstrate the impact of ξ_w on the concentration gradient. The figure illustrates that higher level of ξ_w raises the concentration of the fluid near the left wall and brings it down close to the right wall. This is true owing to the symmetric nature of wall concentration parameter. There is however a point of intersection at the middle of microchannel where the flow is independent of parameter under consideration. This result is very useful for development and management of reverse flow. Additionally, the result obtained in this study coincides with those obtained by Hamza *et al.* (2024c).

The function of ξ_w on the velocity profile is depicted in Figure 3. It is concluded that the effect of temperature acting on the fluid flow made the reverse starts quicker near the upper plate before rising significantly towards the lower plate. Figure 4 illustrates the pattern of fluid motion for varying values of the magnetic parameter M. It is evident that for all considered values of M, there is a decline in the flow pattern. The fundamental cause of this behavior is the availability of a magnetic effect which acts to create a resistivity force (the Lorentz force) that restrains the velocity. Figure 5 explains the variation of the velocity gradient versus

displacement y, and the results obtained is consistent with previously works. It is revealed from this figure that as particles move away from the SHS, their velocity grows briefly before weakens as they reach the middle. Additionally, in the absence of SHS and NSS, the velocity of the fluid experience a sluggish growth and then a steady movement until it reaches the midsection of the microchannel. In all, in the presence of velocity slip and temperature jump, the maximum velocity is attained.

Figure 6 depicts the deviations of chemically reacting parameter λ on the temperature gradient. It is worthy of note as the value of λ rises, the temperature improves substantially. According to Hamza (2016), higher levels of λ representing the chemical reactant parameter, means stronger viscous heating effect, which consequently strengthens the temperature. Similarly, the action of λ is to escalate the fluid velocity in the microchannel as captured in Figure 7. Further, it is noticed that the fluid wall effect lowers as the velocity slip grows at the SHO walls. As a result, the gas moves faster near the wall. A decrease in the fluid viscosity and a subsequent increase in fluid velocity are orchestrated by the significant increase in temperature in response to the increased λ. Figures 8a and b shown the function of ξ_w versus γ on the skin friction coefficient. It is was revealed that growing values of ξ_w promotes the frictional force at the both microchannel plates due to the nature symmetric wall conditions. The action of M at both upstanding walls for skin friction is elucidated in Figures 9a and b. At the wall (y=0), there is a remarkable strengthening in the sheering stress, as demonstrated in Figure 9a, however, at y=1, the contrary effect occurs as plotted in Figure 9b.

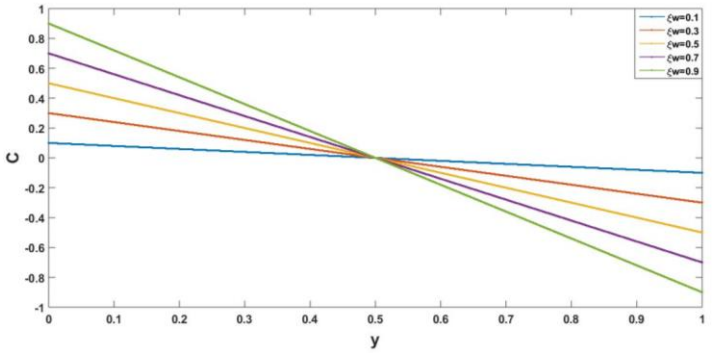


Figure 2: Action of ξ_w on Concentration distribution

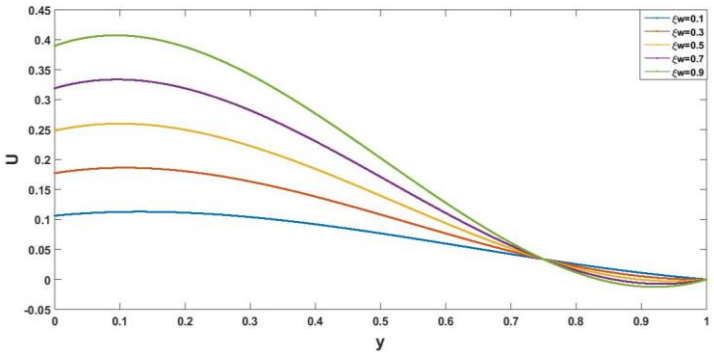


Figure 3: Action of ξ_w on Velocity distribution

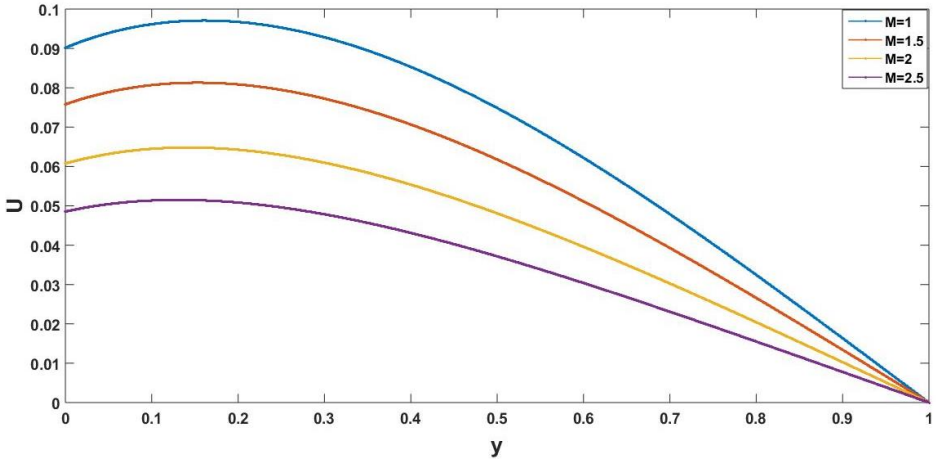


Figure 4: Action of M on velocity distribution

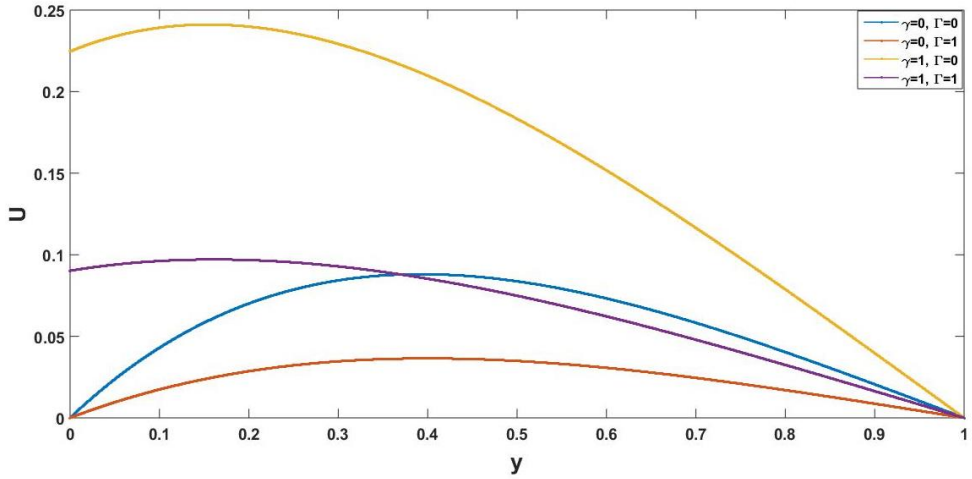


Figure 5: Action of displacement y on velocity distribution

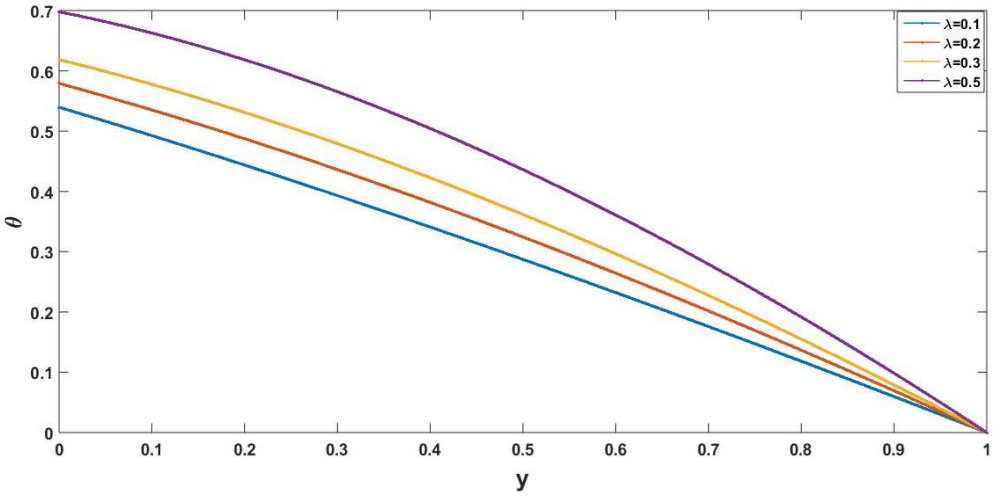


Figure 6: Action of λ on temperature distribution

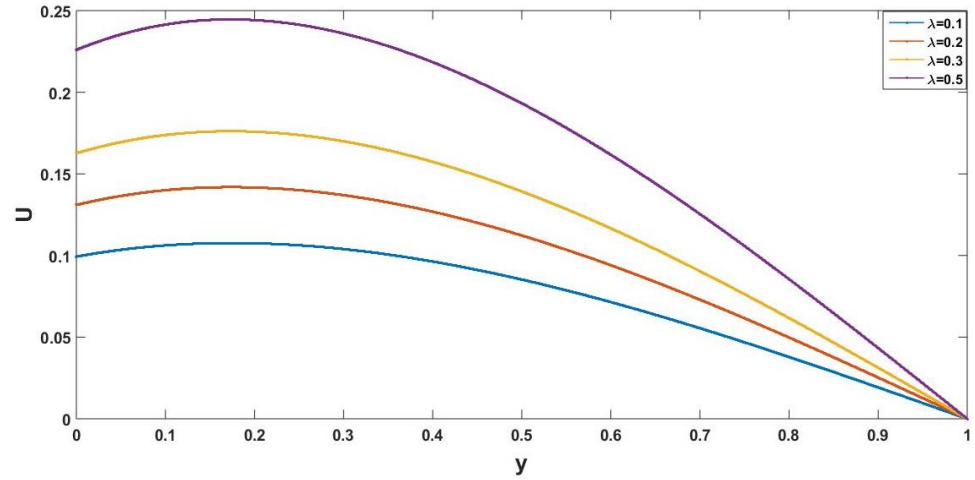


Figure 7: Action of λ on velocity distribution

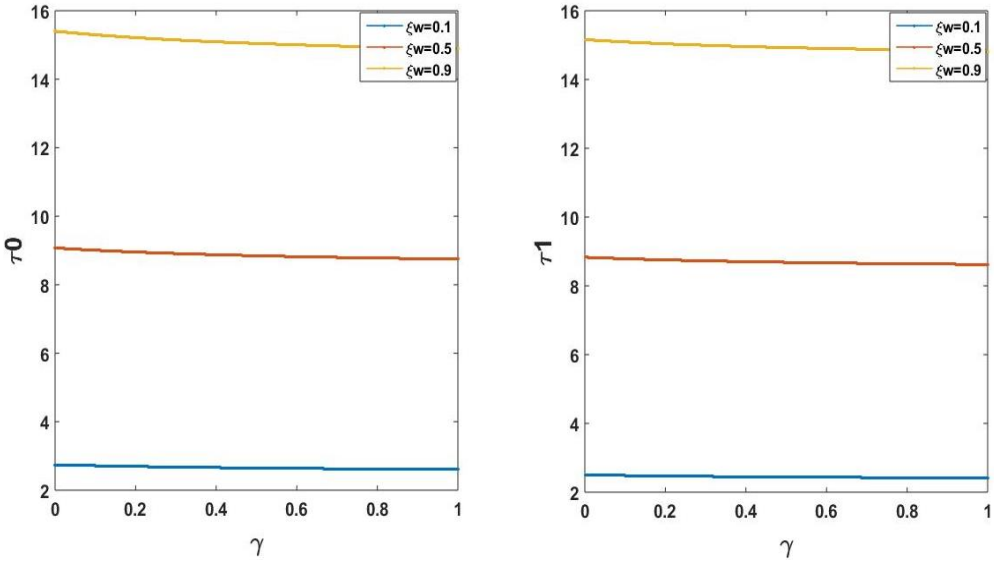


Figure 8: Action of ξ_w on Skin Friction

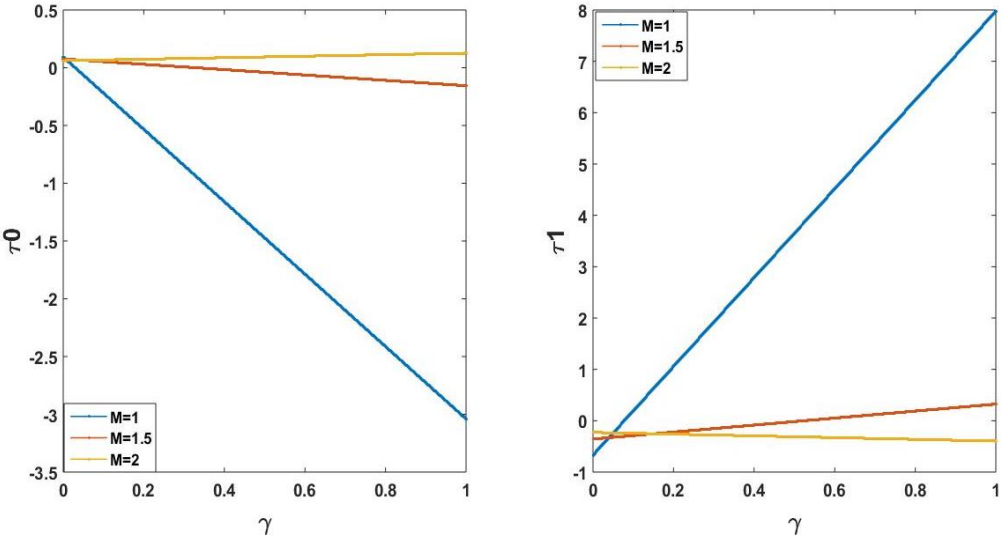


Figure 9: Action of M on Skin Friction

Validation of Results

Setting **N** and ξ_w to be zero respectively, the work of Ojemeri and Onwubuya (2023) is successfully retrieved, establishing a good concurrence between the present study and their work.

Table 1: Demonstrates the numerical comparison of Ojemeri and Onwubuya's (2023) work with the present study for velocity gradient for γ = Γ= 1, M = 1, when $\mathbf{N} = \xi_w = \mathbf{0}$.

Y	**Ojemeri and Onwubuya (2023c)** $\boldsymbol{\gamma} = \Gamma = \mathbf{1}$, $\boldsymbol{\lambda} = \mathbf{0.001}$		**Present work** $\boldsymbol{\gamma} = \Gamma = \mathbf{1}$, $\boldsymbol{\lambda} = \mathbf{0.001}$ $\mathbf{N} = \xi_w = \mathbf{0}$	
	θ (z)	U(z)	θ (z)	U(z)
0.1	0.4500	0.0843	0.4500	0.0843
0.2	0.4000	0.0856	0.4000	0.0856
0.3	0.3500	0.0831	0.3500	0.0831
0.4	0.3000	0.0772	0.3000	0.0772
0.5	0.2500	0.0686	0.2500	0.0686

Conclusion

This research investigated the impact of symmetric wall concentration on Arrhenius-controlled heat and mass transfer flow in a magnetized free convection over a slit microchannel equipped with SHO characteristics. A semi-analytical (regular perturbation) approach is used to treat the novel ordinary differential equations dictating the flow in terms of temperature and velocity components. The influence of key parameters involved in the fluid is demonstrated with the aid of line graphs. For the limiting case ($\mathrm{N} = \xi_w = 0$), this results are compared with previous work, and a very good concurrence exist. Some interesting findings from this paper is outlined below:

i. The velocity and concentration of the fluid are strongly influenced by the action of symmetric wall concentration. Flow reversal is observed as the symmetric wall concentration increase.

ii. The effect of λ is envisaged to improve the fluid's temperature and velocity gradients.

iii. The fluid's velocity and temperature are at their peak by elevating the velocity slip and temperature jump parameters respectively.

iv. It was concluded that higher values of ξ_w parameter improve the skin friction at both plates of the microchannel.

v. The shearing stress is stronger at the surface (y = 0) for mounting level of M, whereas a counter attribute occurs at (y = 1).

vi. In the future, the effects of Darcy porous medium and mixed convection would be studied on this model.

References

Akhtari, M. R. and Karimi, N. (2020). Thermohydraulic analysis of a microchannel with varying superhydrophobic roughness. Applied Thermal Engineering, 172, https://doi.org/10.1016/j.applithermaleng.2020.115147

Hamza, M. M., Ojemeri, G. and Ahmad, S. K. (2023a). Insights into an analytical simulation of a natural convection flow controlled by Arrhenius kinetics in a micro-channel, *Heliyon* 9(2023) e17628, pp. 1-13.

Hamza M. M., Ahmad S. K., Ojemeri G., Usman H. and Shuaibu A. (2023b). Exploring the dynamics of an exothermic chemical reaction controlled by Arrhenius kinetics with Hall effect in a microchannel, *FUDMA Journal of Sciences,* 7(3), 112-124.

Hamza M. M, Ojemeri G. and Ahmad S. K (2023c). Insights into an analytical simulation of a natural convection flow controlled by Arrhenius kinetics in a micro-channel, *Heliyon* 9(2023) e17628, pp. 1-13.

Hamza, M. M., Balarabe A. Y., Ibrahim M., Akpootu D. O. and Sheriff A. (2025). Transient fractional dusty fluid flow in a superhydrophobic microchannel, *European Physical Journal Plus,*140, 366, pp 1-17.

Hamza, M. M., Shehu, A., Muhammad, I., Shuaibu, A., Ojemeri, G. (2024a). Electro-kinetically free convective heat flow in a slit microchannel, *International Journal of Applied and Computational Mathematics,* 10, https://doi.org/10.1007/s40819-024-01765-x

Hamza, M. M., Shehu, A., Muhammad, I., Shuaibu, A., Ojemeri, G. (2024b). Electrokinetically controlled mixed convective heat flow in a slit microchannel, *Heat Transfer,* DOI:10.1002/htj.23104

Hamza, M. M., Bello S. R., Ibrahim Y., Bello A. and Tasiu R. A. (2024c). Casson fluid flow with heat sink affected by symmetric wall temperature and concentration conditions, *Journal of Engineering Technology*, 15(2). https://doi.org/10.54554/jet.2024.15.2.002

Hamza, M. M., Shuaibu, A., Ahmad, S. K. (2022). Unsteady MHD free convection flow of an exothermic fluid in a convectively heated vertical channel filled with porous medium, *Scientific Reports*, 12, 11989.

Hartmann, J. and Lazarus, F. (1937). Hg-dynamics II: theory of laminar flow of electrically conductive liquids in a homogeneous magnetic field, *Matematisk-Fysiske Meddelelser*, 15(7).

Heidarian, A., Rafee, R., Valipour, M. S. (2020). Effects of wall hydrophobicity on the thermohydraulic performance of the microchan nels with nanofluids. Int. Comm. Heat and Mass Transfer, 117, https://doi.org/10.1016/j.icheatmasstransfer.2020.104758

Jawad, M., Saeed, A. and Gul, T. (2021). Entropy generation for MHD Maxwell nanofluid flow past a porous and stretching surface with Dufour and Soret effects, *Braz. J. Phys*, pp. 1-13, htttps://doi.org/10.1007/s13538-020-00835.

Jha, B. K. and Gwandu, B. J. (2018). MHD free convection flow in a vertical slit micro-channel with super-hydrophobic slip and temperature jump: Heating by constant wall temperature. Alexandria Engineering Journal, 57, https:// dx.doi.org/ 10.1016/j.aej.2017.08.022

Jha, B. K. and Gwandu, B. J. (2020). MHD free convection flow in a vertical porous super-hydrophobic microchannel. J. Proc. Mech. Eng., 235 (2).

Jha, B. K., Altine, M. M. and Hussaini, A. M. (2023). MHD steady natural convection in a vertical porous channel in the presence of point/line heat source/sink: An exact solution, *Heat Transfer, Wiley*, pp. 1-15, DOI: 101002/htj.22903.

Lee H., Fridlind A. M. and Ackerman A. S. (2021). An evaluation of size-resolved cloud microphysics scheme numerics for use with radar observations, Part II: condensation and evaporation, J. Atmos. Sci., 78(5), 1629-1645. DOI:10.1175/JAS-D-20-0213.1.

Obalalu, A. M., Ajala, O. A., Adeosun, A. T., Akindele, A. O., Oladapo, O. A., Olajide, O. A. (2021). Significance of variable electrical conductivity on non-Newtonian fluid flow between two vertical plates in the coexistence of Arrhenius energy and exothermic chemical reaction, *Partial Diff. Eqn Appl Math,* 4, 100184, pp. 1-9.

Ojemeri, G. and Onwubuya, I. O. (2023a). Exploring the dynamics of viscous dissipative fluid past a super-hydrophobic microchannel in the coexistence of mixed convection and porous medium, *Saudi Journal of Engineering Technology*, **8**, pp.71-80.

Ojemeri, G. and Onwubuya, I. O. (2023b). Analysis of mixed convection flow on Arrhenius-controlled heat generating/absorbing fluid in a superhydrophobic microchannel: A semi-analytical approach, *Dutse Journal of Pure and Applied Sciences,* 9a**,** 344-357.

Ojemeri G. and Onwubuya I. O. (2023c). Investigation of Arrhenius-controlled chemical reaction through a superhydrophobic microchannel, *FUDMA Journal of Sciences,* 7(3), 80-86.

Ojemeri G. and Onwubuya I. O. (2023d). Significance of viscous dissipation and porosity effects in a heated superhydrophobic microchannel, *Journal of Engineering and Technology (JET),* 14(2), 1-19.

Ojemeri, G. and Hamza, M. M. (2022). Heat transfer analysis of Arrhenius-controlled free convective hydromagnetic flow with heat generation/absorption effect in a micro-channel, *Alexandria Eng. J.*, 61, pp. 12797-12811.

Ojemeri, G., Omokhuale, E., Hamza, M. M., Onwubuya, I. O., Shuaibu, A. (2023a). A Computational Analysis on Steady MHD Casson Fluid Flow Across a Vertical Porous Channel Affected by Thermal Radiation Effect, *Int. J Sci Glob Sus.,* **9**(1), https://doi.org/ 10.57233/ijsgs.v 9i1.393.

Ojemeri, G., Onwubuya I. O., Omokhuale, E., Hussaini A. and Shuaibu, A. (2024). Analytical investigation of Arrhenius kinetics with heat source/sink impacts along a heated superhydrophobic microchannel, UMYU Scientifica, 3(1), 61-71. DOI:105619/usci.2431.004.

Ojemeri, G., Onwubuya I. O., Shuaibu A., Omokhuale, E. and. Altine M. M. (2023c). Arrhenius-controlled heat transfer fluid provoked by porosity effect through a vertical microchannel: An analytical approach, *Continental Journal of Applied Sciences,* 18(1), 18-40.

Omokhuale E. and Dange M. S. (2023). Natural convection Couette flow in the presence of magnetic field and thermal property. International Journal of Science for Global Sustainability, 9(2), 10 – 20. Doi.org/10.57233/ijsgs.v 9i2.453.

Omokhuale E., Ojemeri G., Muhammad A. and Usman H. (2024a). Significance of Viscous Dissipation on Hydromagnetic Oscillatory Flow Affected by Nanoparticles Through a Boundary Layer Regime, International Journal of Development Mathematics 1(1), pp. 098-113.

Omokhuale E., Abubakar J. and Ojemeri G. (2024b). Mixed Convection Flow of a Magnetized Nanofluid with Viscous Dissipation in an Oscillatory System, *International Journal of Science for Global Sustainability*, 10(2), pp. 229-241. DOI: https://doi.org/10.57233/ijsgs.v10i2.672.

Onwubuya I. O., Ojemeri G. and Uko M. A. (2024). Performance Assessment of Viscous Dissipative Fluid Due to Heat Source/Sink in a Slit Microchannel, *International Journal of Science for Global Sustainability,* 10(3), pp. 139-151. DOI: https://doi.org/10.57233/ijsgs.v10i3.710

Onwubuya, I. O. and Ojemeri, G. (2023). Evaluation of mixed convection-radiation flow of a viscous fluid restricted to a vertical porous channel: A comparative Study, *Caliphate Journal Science and Technology*, 5(3), pp. 1-9.

Prakash D. and Sivakumar N. (2018). Influence of viscous and ohmic heating on mhd flow of nanofluid over an inclined nonlinear stretching sheet embedded in a porous medium, *International Journal of Mechanical Engineering and Technology (IJM ET),* 9(8), pp. 992-1001.

Reddy, J. V. R., Kumar, K. A., Sugunamma V., Sandeep, N. (2018). Effect of cross diffusion on MHD non-Newtonian fluids flow past a stretching sheet with non-uniform heat source/sink: A comparative study, *Alexandria Eng. J.* 57(3), pp. 1829–1838.

Rostami H T., Fallah N. M., Hosseinzadeh Kh. and Ganji D. D. (2021). Investigation of mixture-based dusty hybrid nanofluid flow in porous media affected by magnetic field using RBF method, *International Journal Ambient Energy*, DOI: 10.1080/01430750.2021.20230

Saeed, A. and Gul, T. (2021). Bio-convection Casson nano-fluid flow together with Darcy-Forchheimer due to a rotating disk with thermal radiation and Arrhenius activation energy, *SN Applied Science*, **3**, 78.

Sharma, H., Gaddam, A., Agrawal, A., Joshi, S.S. and Dimov, S. S. (2020). Influence of texture shape and arrangement on thermo-hydraulic performance of textured microchannels. Int. J. Therm. Sci., 147, https://doi.org/10.1016/j.ijthermalsci.2019.106146

Sia, G. D., Lim, C.S., Tan, M.K., Chen, G.M. and Hung, Y. M. (2023). Anomalously enhanced subcooled flow boiling in superhydrophobic graphene-nanoplatelets'-coated microchannels. Int. Comm. Heat and Mass Transfer, 146, https://doi.org/ 10.1016/ j.icheatmasstransfer.2023.106932

Sravanthi, C. S., Gorla, R. S. R. (2018). Effects of heat source/sink and chemical reaction on MHD Maxwell nanofluid flow over a convectively heated exponentially stretching sheet using Homotopy analysis method, *Int. J. Appl. Mech. Eng.* 23(1), pp. 137–159.

Uka U. A., Emeziem I. C., Ayinde S. A., Adenika C. and K. O. Agbo (2023). Enhancement of heat transfer with viscous dissipation impact on fluid flow past a moving wedge in a permeable domain, *Eskişehir Technical University Journal of Science and Technology A- Applied Sciences and Engineering*, 24(3), pp. 164-176, DOI:10.18038/estubtda.1197024

Uygun, N. and Ahmad H. T. (2022). Botmart. The effect of Hall parameter on the MHD fluid flow and heat transfer induced by uniform radial electric field due to a shrinking rotating disk. *Case studies in thermal engineering*, 37,102222.

Yale I. D., Uchiri A. M. T., Hamza M. M., and Ojemeri G. (2023). Effect of viscous dissipation fluid in a slit microchannel with heated superhydrophobic surface, *Dutse Journal of Pure and Applied Sciences*, 9(3b), pp. 290-302.

Zhang, W., Wang, Q., Zeng, M., and Zhao, C. (2019). Thermoelectric effect and temperature-gradient-driven electrokinetic flow of electrolyte solutions in charged nanocapillaries. *International Journal of Heat and Mass Transfer, 143, https://*doi:10.1016/ j.ijheatmasstransfer.2019.118569.

Appendix

$$J_1 = -J_2, J_2 = \frac{1}{1+\Gamma}, J_3 = \frac{\left(\frac{1}{2} + \frac{J_1}{6} + \frac{J_2}{2} + a_1\frac{J_1^2}{12} + a_1\frac{J_1 J_2}{3} + a_1\frac{J_2^2}{2}\right)}{1+\Gamma}, J_4 = \Gamma J_3$$

$$J_5 = \gamma[MJ_6 + J_7] - J_8, J_6 = \frac{-\gamma J_8 cosh(M) + J_9 cosh(M)}{\gamma M cosh(M) + si\text{nh(M)}},$$

$$J_8 = \frac{J_1}{M^2}, J_9 = \frac{J_2 + 2J_7}{M^2}, J_{10} = \gamma[MJ_{11} + J_{16}] - J_{17},$$

$$J_{11} = \frac{-a_{10} - a_9}{\gamma M cosh(M) + si\text{nh(M)}}, J_{12} = \frac{-a_3}{M^2}, J_{13} = \frac{-a_4}{M^2}, J_{14} = \frac{(a_3 + 20J_{12})}{M^2},$$

$$J_{15} = \frac{(a_6 + 12J_{13})}{M^2}, J_{16} = \frac{(a_7 + 6J_{14})}{M^2}, J_{17} = \frac{(a_8 + 2J_{15})}{M^2}, a_1 = \frac{1}{2} - \varepsilon,$$

$$a_2 = J_7 + J_8 + J_{9,}\ a_4 = \frac{J_1^2 a_1}{12}, a_5 = \frac{J_1}{6} + \frac{J_1 J_2 a_1}{3}$$

$$a_8 = -J_4\ a_9 = J_{12} + J_{13} + J_{14} + J_{15} + J_{16} + J_{17}, a_{10} = (\gamma J_{16} - J_{17})cosh(M)$$

Nomenclature

$B0$=constant magnetic flux density [kg/s2.m2]

g=gravitational force [m/s2]

h= channel size [m]

CpCv=specific heats at constant pressure and constant volume [Jkg-1K-1]

M= magnetic field [-]

N= Sustention parameter [-]

ξ_w = Symmetric wall concentration [-]

e= activation energy

Nu=dimensionless heat transfer rate [-]

T=dimensionless temperature of the fluid [K]

T0=reference temperature [K]

u=dimensionless velocity of the fluid [ms-1]

y= dimensionless distance between plates

U0=reference velocity [ms-1]

Greek letters

γ = velocity slip parameter (-)
Γ = temperature jump parameter (-)
λ =chemical reacting parameter (-)
β =thermal expansion coefficient [K-1]
μ =variable fluid viscosity [kgm-1s-1]
k=thermal conductivity [m.kg/s3. K]
α =thermal diffusivity [m2s-1]
σ =conductivity of the electric fluid [s3m2/kg]
ρ = fluid density[kgm-3]
v =viscosity of the fluid [m2s-1